Low-Cost Depth-Camera: Open-source 3D displacement measurements for 4D printed hygroscopic composites

Fabio Bianconi [1], Marco Filippucci [1], Giulia Pelliccia [1]*, Gianluca Rossi[2], Tommaso Tocci[2], Giulio Tribbiani[3], David Correa[4]

[1] Department of Civil and Environmental Engineering, University of Perugia, via G. Duranti 93 06125 Perugia, Italy – fabio.bianconi@unipg.it, marco.filippucci@unipg.it, giulia.pelliccia@outlook.it
[2] Department of Engineering, University of Perugia, via G. Duranti 93 06125 Perugia, Italy – gianluca.rossi@unipg.it, tommaso.tocci@outlook.it
[3] Centre of Studies and Activities for Space "Giuseppe Colombo" CISAS, University of Padova, via Venezia 15 35131 Padova, Italy – giulio.tribbiani@studenti.unipd.it
[4] School of Architecture, University of Waterloo, Cambridge (ON), Canada – david.correa@uwaterloo.ca

Technical Commission II

KEY WORDS: 4D printing, Wood Polymer Composites, Depth Camera, Image Analysis, Hygroscopic Actuators, 3D Displacement Measurements

ABSTRACT:

4D printing (4DP) is a growing branch of 3D printing technology that involves the design of composite material architectures capable of shape-change transformations, which occur post printing, in response to external stimulus. Among these, Wood Polymer Composites (WPCs) change their shape in reaction to changes of moisture content, shrinking or swelling like natural wood until the equilibrium with the environment is reached. Such intrinsic material behavior can be particularly useful in the development of passive moisture airflow controllers that can modulate humidity and airflow in indoor environments to improve air quality. Precise measurement of the time-based stimulus induced shape-change response of these composites is critical to assess the responsiveness, velocity of reaction and overall deformation of the designed 4DP composite mechanisms. Up until now, Digital Image Correlation (DIC) techniques have been widely used for such purpose. However, DIC methods require expensive equipment and costly commercial software. This paper presents a Low-Cost Depth-Camera (LCDC) method that uses a free custom algorithm that returns a 3D coloured displacement map with the corresponding meshes of the acquired object. The LCDC method does not require specialized equipment and allows for an overall understanding of the time-dependent deformation of 4DP actuators, this method also facilitates the comparison between composites with different properties under the same external conditions. This new LCDC method has the potential to further 4DP research by providing an open-source, accessible and reliable tool to assess 3D displacement measurements.

1. INTRODUCTION

Hygroscopic actuators have great potential to improve indoor building comfort through their climate adaptive behaviour as they don't require failure prone electronic controllers and actuators. Previous research on 4DP of hygromorphs has been focused on the application of such properties for shape-change transformations in relation to self-assembly (Campbell et al., 2014:), biological role models (Poppinga et al., 2020:), wearable systems (Cheng et al., 2021:), among many others. However, their use in passive moisture airflow controllers have not yet been thoroughly explored.

Over the last 10 years 3D printing (3DP) has been widely adopted for various areas of application (Mustapha and Metwalli, 2021:). Fused Deposition Modelling technology (FDM) is the most widely adopted 3DP technology as it has many advantages compared to other fabrication methods, most notably, lower costs (Ni et al., 2017:). In the fabrication of sensors and actuators, in particular, 3DP is being used taking advantage of specific Stimulus Responsive Materials (SRM) (Tibbits, 2013:) and hygroscopic material architectures (Correa, 2022:).

3DP has a wide variety of applications (Khosravani and Reinicke, 2020:) and its customizability makes it suitable to be also used in unconventional ways. By introducing the fourth dimension of time, for example, 4D printing enables the fabrication of composites that change their configurations in response to a stimulus such as light, heat, solvents, electricity or water (Pei, 2014:; Zolfagharian et al., 2016:). The reaction to the specific stimulus can be pre-programmed to respond to user needs or environmental changes (Tibbits, 2014:). Different thermoplastic filaments can be used to achieve such SRM behaviour. Wood Polymer Composites (WPC) filaments, which contain between 20% and 40% wood flour in a polymer matrix (usually PLA), are commercially available and therefore one of the most widely used (Correa et al., 2020:; Spear et al., 2015:). Such filament is particularly used in 4DP applications due to its hygroscopic swelling properties. Just like natural wood, WPCs react to changes in humidity by absorbing/desorbing moisture from the environment (Correa Zuluaga and Menges, 2015:; Le Duigou and Castro, 2015:).

Precise manipulation of toolpaths, raster patterns, material layering and printing properties are necessary to design 4DP WPCs (Vazquez et al., 2019:). The specific material architecture needs to be composed of at least two functional layers whose

* Corresponding author

difference in the expansion coefficient results in the stress induced bending of the composite (Le Duigou and Correa 2022). The expansion layer has a high hygroscopic swelling coefficient that leads to dimensional changes in response to relative humidity fluctuations. The constraint layer, instead, is non-hygroscopic or less hygroscopic than the first one; its purpose is to contrast the shrinking/swelling of the expansion layer to induce bending. Therefore, the reaction of such actuators is strictly dependent on specific printing settings, such as raster pattern, layer height, extrusion rate, etc. For instance, the layer height defines the thickness of the expansion and the constraint layer while the raster pattern defines the primary direction of swelling. By adapting Timoshenko's theory for bimetallic strips (Timoshenko, 1925:) to hygro-responsive bilayers, it was observed that what actually affects the responsiveness of the actuator is the ratio between the thickness of the constraint layer and the expansion one, rather than the overall thickness of the composite (Erb et al., 2013:; Reichert et al., 2015:; Rüggeberg and Burgert, 2015:; Wood et al., 2018:). The latter, in fact, mostly involves the time required to complete the absorption-desorption cycle. The raster pattern is a second relevant parameter which concerns the type of print-path design, the direction and orientation of each printed filament in relation to each other, used to discretize the geometries and its density. The raster pattern defines the dominant direction of swelling/shrinking in the expansion layer and the appropriate direction and effectiveness of the constraint one.

The ability of 4DP WPC mechanisms to use its intrinsic material properties to change shape in response to relative humidity offers great potential to develop passive environmental control mechanisms for building comfort applications. These applications might involve outdoor façade mechanisms, in direct contact with precipitation, or indoor ventilation louvers that respond to occupant driven changes in relative humidity. However, the assessment of such responsive behaviour requires a measurement method able to track and compare the displacements of multiple composite samples. This kind of evaluation can be done through conventional image analysis techniques (Xhimitiku et al., 2021:), such as Digital Image Correlation (Montanini et al., 2020:; Pan et al., 2009:). The use of a stereovision 3D DIC technique with commercial software can involve considerable costs due to the specific equipment and software licensing.

Another type of image analysis based on a contactless 3D shape measurement technique is photomodelling (Bianconi et al., 2017:; Calalucci et al., 2018:). In this technique feature detection algorithms are exploited to reconstruct point clouds and then extrapolate a mesh of the scanned object. Although this method can be inexpensive and frees the user from the need of stereo-calibrate the cameras, it requires a large number of photographs taken from different angles, making it unsuitable for time-varying displacement measurements. In order to simplify the experimental setup and lower costs, a structured light projection technology (Xhimitiku et al., 2019:) was used to perform the 3D shape reconstruction of the 4DP WPC sample. The light projected onto the object is reflected from its surface, then captured by the camera array. By evaluating the way the surface deforms the reflected pattern, it is possible to triangulate the x-y-z position of the object points. Structured light measurement techniques differ depending on the type of electromagnetic radiation emitted: it is possible to project light within the visible spectrum, but also to project infrared (IR) patterns.

An Intel RealSense SR305 Low-Cost Depth Camera (LCDC) based on IR structured light (Zabatani et al., 2020:) was used. By implementing simple code written in Python that communicates with the depth camera SDK and uses methods of point clouds and meshes extrapolation, it was possible to measure the displacements of the 4DP actuators to obtain a spatial map of the displacements correlated to time. The use of a single camera makes the test bench cheaper and avoids the tedious procedure of stereo calibration.

2. MATERIALS AND METHODS

2.1 Programming the material architecture of 4DP hygroscopic actuators

The best configurations and printing properties were identified to maximize the deformation in the shortest time. This process depends on the precise deposition of material on the printing bed and can be controlled through a specially developed visual scripting algorithm. The script allows for an overall customization of the designed print paths and the corresponding printing parameters that influence the final deformation of the composite. By coupling two main layers with different hygroscopic coefficients a stress is induced when a variation in environmental humidity occurs. Furthermore, to ensure an accurate adhesion between the two main layers, z-offsets and printing speed were adjusted. Through these parameters delamination due to the coupling of different thermoplastic materials was avoided, which is particularly important when considering long-term behavior. The design of the material architecture, and subsequent effect in its mechanical properties and hygroscopic behaviour, are implemented through the computational script. This design tool, made in Grasshopper, gives precise control of each of these variables individually and allows any geometry to be discretized through the specific pattern chosen according to the type of layer and the material used. This custom computational design tool is distinctly different from ordinary slicing softwares, which only provide a limited access to some of these parameters. While a slicer operates as a black box focusing only on print quality (consistency and surface quality), the computational tool gives open access to all printing parameters. For this research, print quality is secondary to the definition of the printing principles that characterize an optimal hygroscopic actuator.

The 4DP sample used for the displacement measurements was printed using a Prusa i3 MK3S+ with a 0.4 mm nozzle diameter. The hygro-responsive behavior of the composite was designed considering the stress-induced bending achieved through the particular bilayer architecture. The active layer was printed with the wood-based filament with a zig-zag pattern and 0.4 mm layer height, while for the constraint one PLA was chosen with a grid pattern and 0.2 mm layer height. A third type of layer called bonding was in this case necessary to further improve the adhesion between the wooden filament and PLA.

The actuator can be considered as an example of a kirigami application, which is a traditional Japanese technique that, contrary to origami, also involves cutting. This concept has been recently developed and applied to composite materials to transform 2D elements in more complex 3D geometries (Xu et al., 2017:). Instead of assembling the constituent parts of the final object, this approach enables continuous and direct 2D-to-3D transformations (Chen et al., 2020:). Therefore, the responsive composite can be made from a single printing process. For the printed prototype presented in this paper a thin frame was used as a support base for four triangular flaps. The flaps were

originally printed in a unique part which was then cut through a heat cutter. The hygro-responsive parts bend inwards when humidity increases and outwards when it decreases, while they show a flat configuration when humidity is around 40-50% (Fig. 1). This range was observed to be the optimal for the well-being of the occupants. On the one hand, below 30% there may be problems of desiccation of the mucous membranes, while values above 60% may increase the development of mites of dust (Wolkoff and Kjærgaard, 2007:). On the other, humidity values higher than 70% increase the sensation of hot with high temperatures (Buonocore et al., 2018:). Moreover, kirigami technique was particularly useful to ensure a complete closure of the responsive parts once humidity levels return to the optimal environmental values, as the actuator goes back to the original configuration it had before cutting.

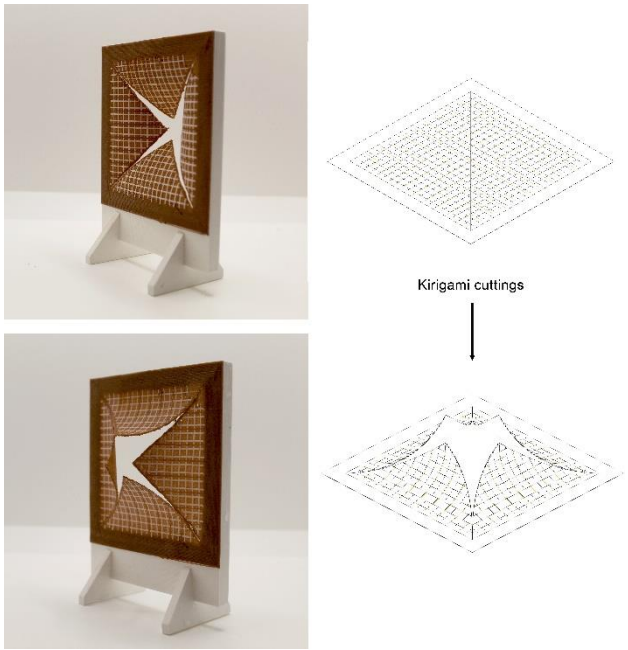

Figure 1. The kirigami technique allows the mechanism to open and close for different levels of humidity.

2.2 Displacement measurements

2.2.1 Experimental set-up: A RealSense SR305 Depth Camera, capable of providing both depth maps and RGB images of the framed scene, was used to perform the 3D scanning of the hygroscopic actuator (Fig. 2). To generate such depth maps the camera exploits a dedicated module, consisting of an infrared fringe projector and an IR camera that captures the reflection of such fringes on the scene. The maps are then recomputed by a processor, which overlays colour photographs of the scene with depth information.

4DP WPCs show a quicker responsiveness to humidity when they are submerged in water rather than exposed to environmental relative humidity. To achieve full deformation the specimen was therefore immersed for several hours; however, performing the scans with the specimen dipped into water, inside a glass case, leads to optical problems in terms of air-water refractive index change. To overcome this issue, the depth maps were acquired while the specimen was drying. It is also known that the desorption cycle is faster than the absorption one (Jain and Kurhekar, 2015:), therefore the fastest way to run the acquisitions is during the drying cycle. A 3DP plastic frame was made to mainly focus the attention of the measurement on the deformation of the inner part of the specimen, thus blocking its edges. Since the acquisitions were made with both the LCDC and the sample support structure both fixed, it was not necessary to implement point cloud alignment algorithms, as those were automatically overlaid.

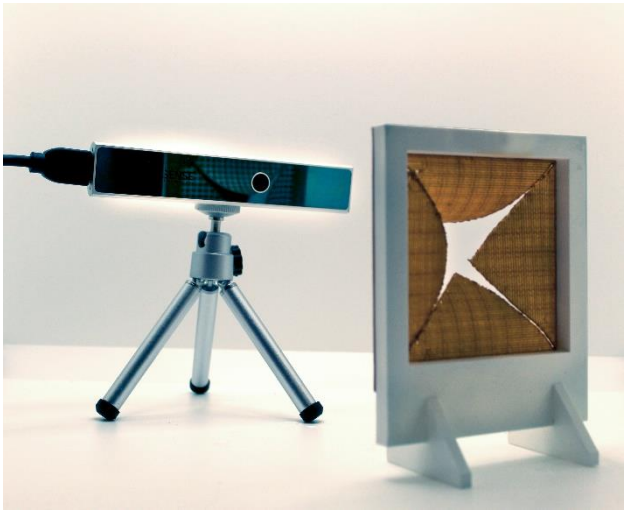

Figure 2. The RealSense SR305 Depth Camera was put in front of the actuator to acquire its passive motion.

2.2.2 Displacement measuring process: The results of the scans were depth maps of the sample at different time instants throughout the drying process. These maps consisted of a series of pixels, each containing the distance in millimeters of the portion of the scene framed by it. In order to perform the displacement measurement, it was necessary to derive point clouds from these maps, hence the meshes.
An algorithm capable of obtaining the 3D coordinates of a point in the scene was used to obtain the point clouds by knowing the intrinsic and extrinsic parameters of the LCDC. The extrinsic factors consist of the matrix resulting from the product between the rotation matrix R and the translation vector t and are needed to bring the reference system of the scene back to that of the camera. Intrinsic factors, on the other hand, are necessary to move from the camera reference system to the image reference system. Given u, v and d respectively the coordinates and the distance information of the pixel, cx, cy the coordinates of the optical center of the camera, and fx, fy the focal lengths (expressed in pixels), the algorithm implements the following relations to obtain the x, y, z coordinates of the points:

$$z = d \tag{1}$$

$$x = \frac{u - c_x}{f_x} \tag{2}$$

$$y = \frac{v - c_y}{f_y} \tag{3}$$

The second step was to obtain the meshes, starting from the point clouds previously generated. The mesh creating algorithm implements the Ball Pivoting Algorithm (BPA) (Bernardini et al., 1999:). Given a point cloud and a sphere with radius ρ, whose

value is set according to the geometry to be meshed, the BPA consist in two simple step: keeping the sphere in contact with two point, it is pivoted until it touches another point. The process is repeated, pivoting the ball around each edge of the current mesh boundary. The triplets of point touched by the ball are the vertices of the new triangles; hence the set of triangles constitutes the interpolating mesh. The radius value ρ has to be carefully decided: setting it to low means not being able to reach a new point during the pivoting, therefore having holes in the mesh; a too high a value would result in failure to detect features if the local curvature of the sample is too high.

The third and final step was to compute the distance of two meshes, therefore the displacement measurement of the sample during the drying process. This displacement was found using a KDTree algorithm that computes the distance from every vertex point in the reference mesh to its closest vertex point in the analyzed mesh. The result is a displacement map of every vertex of the mesh during the deformation process of the sample.

3. RESULTS AND DISCUSSION

The final coloured meshes obtained after the acquisition and processing of the displacements are highly connotative of the overall behavior of the actuator during the drying cycle. The LCDC was set to acquire one frame per minute for six hours and the results were extracted every 60 frames to consider the displacements every hour. In the first two hours an additional step at 90 minutes was considered, as the displacements have a decreasing speed (Fig. 3).

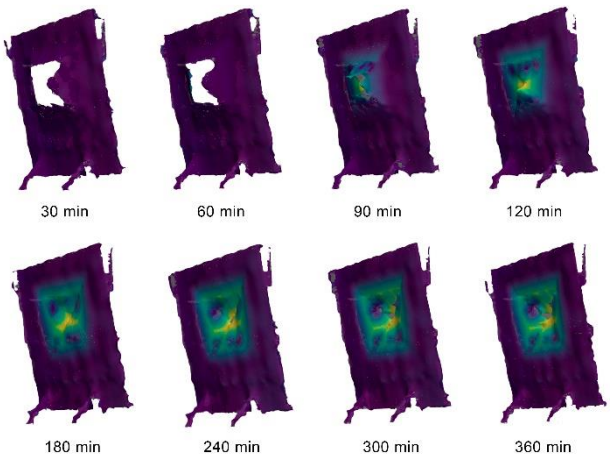

Figure 3. The LCDC acquisitions show the meshes with the coloured map corresponding to the different displacements.

The algorithm applies a coloured map on the mesh depending on the displacement that each pixel undergoes in relation to the frame zero. Figure 4 shows the processed meshes: in the first 60 minutes only one flap undergoes a significant displacement, which can denote a different printing quality between the four flaps. In particular, the left one starts form a higher level of initial curvature in the humid state, compared to the others. Therefore, having a higher moisture content, the drying process starts earlier and faster as the moisture gradient with the environmental humidity is greater for this particular flap. During printing, the adhesion between the constraint layer and the expansion one was slightly compromised in three flaps compared to the left one. This can depend on several factors, such as a not perfect levelling of the printing bed. Although 3DP is a controlled process where algorithms are programmed to optimize and make prints as homogeneous as possible, little errors can result in a considerable different behavior for a 4DP actuator. The LCDC method used in this paper thus allows not only to represent and analyze the overall displacements, but also to easily detect those printing defects.

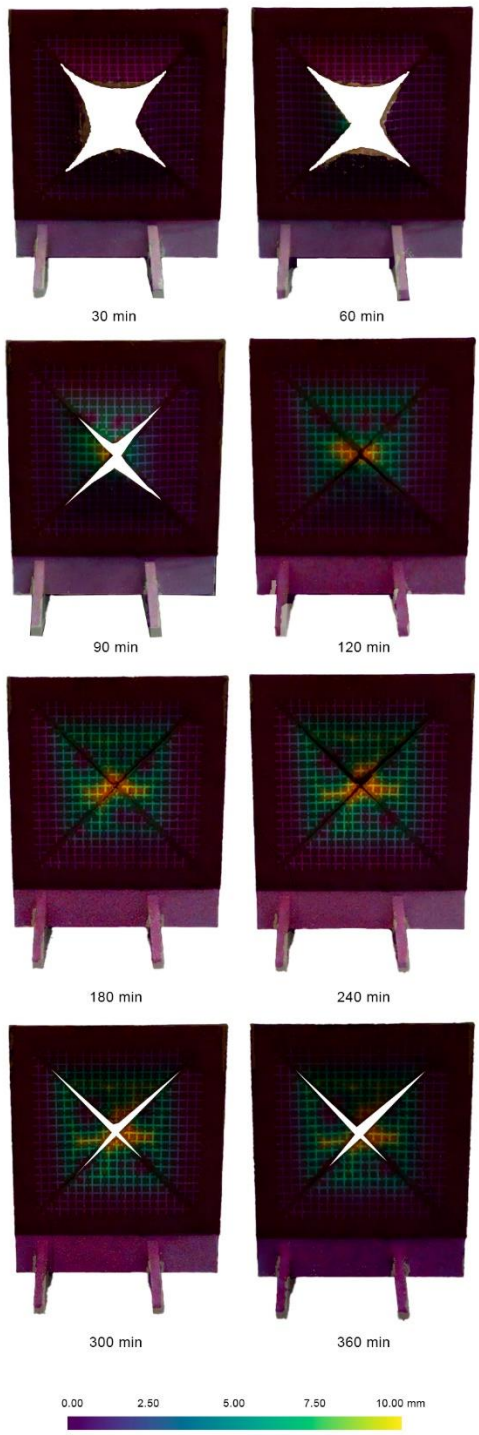

Figure 4. From the front view of the acquisition overlying the textured map of the actuator the punctual differences in the displacements can be noticed.

After 120 minutes the four flaps almost appear completely closed, as the most responsive one has nearly completed its drying cycle, while the three others still need 60 more minutes to reach the flat configuration. It is thus observed that the drying cycle from the initial saturated condition to the flat original one is completed after 180 minutes. Since the environment where the acquisitions were conducted is dryer than the equilibrium moisture value for the actuators, the displacements continue on the opposite direction, as the expansion layer starts shrinking. After 240 minutes this reverse bending is already noticeable and after 360 minutes the equilibrium can be considered achieved.

The overall displacements can thus be evaluated with a maximum of 10 mm in the center of the actuator. The histogram in Figure 5 shows the distribution of the displacement values during the drying cycle. Displacements between 2 and 4 mm are the most frequent during all the acquisition period.

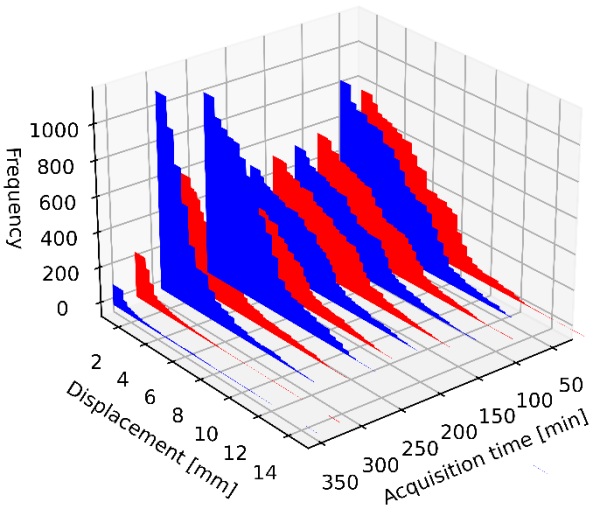

Figure 5. Changing over time (30 minutes steps) of the displacement values distributions during the drying process of the sample.

4. CONCLUSION

The presented research is aimed at assessing 4DP WPCs responsiveness to humidity using a LCDC. Displacement measurements are needed to evaluate the differences between similar hygroscopic actuators and, therefore, understand which printing properties and which materials are most suitable for a fast actuation. Considering the final goal of the research, which is aimed at developing 4DP WPCs passive moisture airflow controllers, this approach is particularly convenient as, compared to other DIC techniques, is low-cost and based on free and customized algorithms.

Through a LCDC the complex multi-directional shape-change transformation of hygroscopic actuators can be better understood due to the improved method of motion tracking. This method does not require the sample to undergo special coating or treatment prior to analysis. In particular, the acquisition returns not only displacement information, but also a 3D digital representation of all the configurations during deformation. The coloured maps applied to the resulting meshes allow the comparison of the responsive behavior between different actuator but also between different parts of the same composite.

In future research LCDC could be used to correlate the displacement to specific changes in the relative humidity of the surrounding environment. This could improve the overall understanding of the deformations applied to a tangible case study of a humid indoor environment.

REFERENCES

Bernardini, F., Mittleman, J., Rushmeier, H., Silva, C., Taubin, G., 1999: The ball-pivoting algorithm for surface reconstruction. *IEEE Trans. Vis. Comput. Graph.* 5, 349–359. https://doi.org/10.1109/2945.817351.

Bianconi, F., Catalucci, S., Filippucci, M., Marsili, R., Moretti, M., Rossi, G., Speranzini, E., 2017: Comparison between two non-contact techniques for art digitalization. *J. Phys. Conf. Ser.* 882, 12005. https://doi.org/10.1088/1742-6596/882/1/012005.

Buonocore, C., De Vecchi, R., Scalco, V., Lamberts, R., 2018: Influence of relative air humidity and movement on human thermal perception in classrooms in a hot and humid climate. *Build. Environ.* 146, 98–106. https://doi.org/10.1016/j.buildenv.2018.09.036.

Campbell, T.A., Tibbits, S., Garrett, B., 2014: The Next Wave: 4D Printing. Programming the Material World. Washington, DC.

Catalucci, S., Marsili, R., Moretti, M., Rossi, G., 2018: Point cloud processing techniques and image analysis comparisons for boat shapes measurements. *Acta IMEKO* 7, 39–44. https://doi.org/10.21014/acta_imeko.v7i2.543.

Chen, S., Chen, J., Zhang, X., Li, Z.-Y., Li, J., 2020: Kirigami/origami: unfolding the new regime of advanced 3D microfabrication/nanofabrication with "folding." *Light Sci. Appl.* 9. https://doi.org/10.1038/s41377-020-0309-9.

Cheng, T., Thielen, M., Poppinga, S., Tahouni, Y., Wood, D., Steinberg, T., Menges, A., Speck, T., 2021: Bio-Inspired Motion Mechanisms: Computational Design and Material Programming of Self-Adjusting 4D-Printed Wearable Systems. *Adv. Sci.* 8, 2100411. https://doi.org/10.1002/ADVS.202100411.

Correa, D., 2022: 4D printed hygroscopic programmable material architectures. University of Stuttgart. ISBN: 978-3-9819457-9-9.

Correa, D., Poppinga, S., Mylo, M.D., Westermeier, A.S., Bruchmann, B., Menges, A., Speck, T., 2020: 4D pine scale: Biomimetic 4D printed autonomous scale and flap structures capable of multi-phase movement. *Philos. Trans. R. Soc. A Math. Phys. Eng. Sci.* 378. https://doi.org/10.1098/rsta.2019.0445.

Correa Zuluaga, D., Menges, A., 2015: 3D printed hygroscopic programmable material systems, in: Materials Research Society Symposium Proceedings. Materials Research Society, pp. 24–31. https://doi.org/10.1557/opl.2015.644.

Erb, R.M., Sander, J.S., Grisch, R., Studart, A.R., 2013: Self-shaping composites with programmable bioinspired microstructures. *Nat. Commun.* 4. https://doi.org/10.1038/ncomms2666.

Jain, S.K., Kurhekar, S.P., 2015: Water absorption and desorption characteristics of wood. *Int. J. Agric. Eng.* 8, 244–247. https://doi.org/10.15740/HAS/IJAE/8.2/244-247.

Khosravani, M.R., Reinicke, T., 2020: 3D-printed sensors: Current progress and future challenges. *Sensors Actuators A Phys.* 305, 111916. https://doi.org/10.1016/J.SNA.2020.111916.

Le Duigou, A., Castro, M., 2015: Moisture-induced self-shaping flax-reinforced polypropylene biocomposite actuator. *Ind. Crops Prod.* 71, 1–6. https://doi.org/10.1016/j.indcrop.2015.03.077.

Montanini, R., Rossi, G., Quattrocchi, A., Alizzio, D., Capponi, L., Marsili, R., Giacomo, A. Di, Tocci, T., 2020: Structural characterization of complex lattice parts by means of optical non-contact measurements. *I2MTC 2020 - Int. Instrum. Meas. Technol. Conf. Proc.* https://doi.org/10.1109/I2MTC43012.2020.9128771.

Mustapha, K.B., Metwalli, K.M., 2021: A review of fused deposition modelling for 3D printing of smart polymeric materials and composites. *Eur. Polym. J.* 156, 110591. https://doi.org/10.1016/J.EURPOLYMJ.2021.110591.

Ni, Y., Ji, R., Long, K., Bu, T., Chen, K., Zhuang, S., 2017: A review of 3D-printed sensors. *http://dx.doi.org/10.1080/05704928.2017.1287082* 52, 623–652. https://doi.org/10.1080/05704928.2017.1287082.

Pan, B., Qian, K., Xie, H., Asundi, A., 2009: Two-dimensional digital image correlation for in-plane displacement and strain measurement: a review. *Meas. Sci. Technol.* 20, 062001. https://doi.org/10.1088/0957-0233/20/6/062001.

Pei, E., 2014: 4D printing: Dawn of an emerging technology cycle. *Assem. Autom.* 34, 310–314. https://doi.org/10.1108/AA-07-2014-062/FULL/PDF.

Poppinga, S., Correa, D., Bruchmann, B., Menges, A., Speck, T., 2020: Plant movements as concept generators for the development of biomimetic compliant mechanisms, in: Integrative and Comparative Biology. Oxford University Press, pp. 886–895. https://doi.org/10.1093/icb/icaa028.

Reichert, S., Menges, A., Correa, D., 2015: Meteorosensitive architecture: Biomimetic building skins based on materially embedded and hygroscopically enabled responsiveness. *Comput. Des.* 60, 50–69. https://doi.org/10.1016/J.CAD.2014.02.010.

Rüggeberg, M., Burgert, I., 2015: Bio-Inspired Wooden Actuators for Large Scale Applications. *PLoS One* 10, e0120718. https://doi.org/10.1371/journal.pone.0120718.

Spear, M.J., Eder, A., Carus, M., 2015: Wood polymer composites. *Wood Compos.* 195–249. https://doi.org/10.1016/B978-1-78242-454-3.00010-X.

Tibbits, S., 2014: 4D Printing: Multi-Material Shape Change. *Archit. Des.* 84, 116–121. https://doi.org/10.1002/AD.1710.

Tibbits, S., 2013: The emergence of 4D printing, in: TED Conference.

Timoshenko, S., 1925: Analysis of Bi-Metal Thermostats. *JOSA, Vol. 11, Issue 3, pp. 233-255* 11, 233–255. https://doi.org/10.1364/JOSA.11.000233.

Vazquez, E., Gürsoy, B., Duarte, J.P., 2019: Formalizing shape-change: Three-dimensional printed shapes and hygroscopic material transformations: *https://doi.org/10.1177/1478077119895216* 18, 67–83. https://doi.org/10.1177/1478077119895216.

Wolkoff, P., Kjærgaard, S.K., 2007: The dichotomy of relative humidity on indoor air quality. *Environ. Int.* https://doi.org/10.1016/j.envint.2007.04.004.

Wood, D., Vailati, C., Menges, A., Rüggeberg, M., 2018: Hygroscopically actuated wood elements for weather responsive and self-forming building parts – Facilitating upscaling and complex shape changes. *Constr. Build. Mater.* 165, 782–791. https://doi.org/10.1016/J.CONBUILDMAT.2017.12.134.

Xhimitiku, I., Bianchi, F., Proietti, M., Tocci, T., Marini, A., Menculini, L., Termite, L.F., Pucci, E., Garinei, A., Marconi, M., Rossi, G., 2021: Anomaly detection in plant growth in a controlled environment using 3D scanning techniques and deep learning. *2021 IEEE Int. Work. Metrol. Agric. For.* 86–91. https://doi.org/10.1109/MetroAgriFor52389.2021.9628481.

Xhimitiku, I., Rossi, G., Baldoni, L., Marsili, R., Coricelli, M., 2019: Critical analysis of instruments and measurement techniques of the shape of trees: Terresrial Laser scanner and Structured Light scanner. *2019 IEEE Int. Work. Metrol. Agric. For. MetroAgriFor* 339–343. https://doi.org/10.1109/MetroAgriFor.2019.8909215.

Xu, L., Shyu, T.C., Kotov, N.A., 2017: Origami and Kirigami Nanocomposites. *ACS Nano* 11, 7587–7599. https://doi.org/10.1021/acsnano.7b03287.

Zabatani, A., Surazhsky, V., Sperling, E., Moshe, S. Ben, Menashe, O., Silver, D.H., Karni, Z., Bronstein, A.M., Bronstein, M.M., Kimmel, R., 2020: Intel® RealSense™ SR300 Coded Light Depth Camera. *IEEE Trans. Pattern Anal. Mach. Intell.* 42, 2333–2345. https://doi.org/10.1109/TPAMI.2019.2915841.

Zolfagharian, A., Kouzani, A.Z., Khoo, S.Y., Moghadam, A.A.A., Gibson, I., Kaynak, A., 2016: Evolution of 3D printed soft actuators. *Sensors Actuators A Phys.* 250, 258–272. https://doi.org/10.1016/J.SNA.2016.09.028.